Water and polypeptide conformations in the gramicidin channel
A molecular dynamics study

See-Wing Chiu,* Shankar Subramaniam,‡ Eric Jakobsson,* and J. Andrew McCammon‡§
*Department of Physiology and Biophysics and Program in Bioengineering, University of Illinois, Urbana, Illinois 61801; ‡Department of Chemistry, University of Houston, Houston, Texas 77204-5641; and §Department of Physiology and Molecular Biophysics, Baylor College of Medicine, Houston, Texas 77030

ABSTRACT Theoretical studies of ion channels address several important questions. The mechanism of ion transport, the role of water structure, the fluctuations of the protein channel itself, and the influence of structural changes are accessible from these studies. In this paper, we have carried out a 70-ps molecular dynamics simulation on a model structure of gramicidin A with channel waters. The backbone of the protein has been analyzed with respect to the orientation of the carbonyl and the amide groups. The results are in conformity with the experimental NMR data. The structure of water and the hydrogen bonding network are also investigated. It is found that the water molecules inside the channel act as a collective chain; whereas the conformation in which all the waters are oriented with the dipoles pointing along the axis of the channel is a preferred one, others are also accessed during the dynamics simulation. A collective coordinate involving the channel waters and some of the hydrogen bonding peptide partners is required to describe the transition of waters from one configuration to the other.

INTRODUCTION

Considerable interest has been evinced in recent years in the theoretical study of ion movement through transmembrane channel proteins. A channel of particular interest for theoretical studies is gramicidin A (1), which is one of the simplest ion channel proteins. Gramicidin A, whose normal channel form is a polypeptide dimer of two beta helices linked to each other head to head by hydrogen bonds, is well studied in both its electrophysiology (2, 3) and structure (4). Being small and relatively simply structured, it serves as an excellent window into the study of microscopic mechanisms involved in membrane transport. Because an ion channel must form an aqueous region spanning the membrane, an issue of primary importance is to understand the water-protein structures and interactions in this region. A number of questions concerning this can be posed, including whether the water forms an icelike lattice through which the ion winds in a labyrinthine fashion, or if the water plays a more active role in facilitating the motion of the ion. To answer these questions, even if only in part, it is inevitable that one has to consider the dynamics of the situation. In the first part of the study we propose to investigate, using the techniques of molecular dynamics (5), the structure and dynamics of the channel, with emphasis on the backbone, and of water inside the channel. In subsequent studies we will focus on the ion transport itself and the side chain orientation and dynamics of the residues.

Gramicidin A has been the subject of some earlier theoretical simulations. Jordan et al. have treated the channel as a simplified dipole helix and have done both molecular mechanics and dynamics simulations (6). Mackay et al. have carried out a dynamics simulation with a complete molecular structure (7). Kim et al. have carried out Monte Carlo simulation on the channel, with special emphasis on the water structure inside the channel (8). Roux and Karplus have done a normal mode analysis on the channel in the absence of waters (9). More recently, Skerra and Brickman have done extensive analysis on dynamics simulations of a simplified model gramicidinlike helix (10, 11). A more extensive review of theoretical gramicidin work is given in Jordan (1). The focus of many studies has been coordination of the ion and the energetics of ion transport. The structure of the channel water itself has been featured in one paper (12). In this paper we provide new data and analyses of the structure and dynamics of the channel backbone and channel water.

In our simulations, we consider the channel in its entire molecular detail and consider channel waters with water caps at either end. To mimic the effects of the lipid membrane and to preserve the global structure of the beta helices, we use a nonelastic time relaxation restraint on the protein. The simulation details are described in the next section. From the simulation, we probe the water structure inside the channel and the mutual influences of the water and protein backbone on each other. We compare our simulations with previous simulations to highlight both the similarities and the differences.

SIMULATION DETAILS

The gramicidin model of Koeppe and Kimura is used as a starting point in our simulation (reference 13 for the backbone and Koeppe, R.E. [personal communication] for side groups). In this model, the two pentadecapeptides are linked head to head with the C—O and N—H bonds (and hence the amide planes), being nearly parallel to the channel axis. This structure for the backbone is slightly different from that proposed by Venkatachalam and Urry (14). Later in the paper, we will present evidence that our results are not very sensitive to the precise choice of starting configuration. To reduce the possibility of any spurious correlations, a random initial configuration of nine channel waters is chosen. A random configuration of a cap of seven waters is placed at each end of the channel. The total number of atoms included in the dynamics simulation (water and protein) is 387. We use a united atom model for methine, methylene, and methyl groups.

The empirical potential energy function used is that from the GROMOS package (15). It comprises terms for bond angles, dihedral angles, improper dihedrals, Lennard-Jones, and electrostatic interactions. Bond lengths are fixed at ideal values by using the SHAKE algorithm (16). The SPC model is used for the waters (15). Calculations were done on the microVax II in the lab of Dr. Jakobsson, the Vax 8650 at the University of Houston, and the CRAY XMP computer at the National Center for Supercomputing Applications (Urbana, IL), using a modified version of the program GROMOS provided by Wilfried van Gunsteren. A routine to add a nonelastic restraint during dynamics was added to mimic the natural constraints imposed by the lipid on the channel protein. The constraint is restricted to all the protein atoms. The net result of using this nonelastic restraint on the system is a first order relaxation of position, given the reference position r_o, so that

$$\frac{dr}{dt} = \frac{(r_o - r)}{\Gamma_r},$$

where Γ_r is the relaxation time ($\Gamma_r \gg$ the time step Δt). In our computations, the relaxation time was 10 ps and the reference positions were those of Koeppe-Kimura (13). The modification to the equations of motion is such that local disturbances are minimized whereas global effects are conserved (17).

Two sets of MD simulations were performed, one with the channel waters and the other without. In both simulations, the system under consideration was carefully equilibrated after initial steepest descent energy minimization. The minimized structure was allowed to equilibrate by assigning random Maxwellian velocities to the atoms and allowing the system to evolve by molecular dynamics simulation for 0.2 ps after each assignment. Assignment temperature and equilibration periods were 50 K (4 ps), 100 K (4 ps), 150 K (4 ps), 200 K (4 ps), 250 K (4 ps), and 300 K (4 ps). Another 4 ps of dynamics was performed without any reassignment to ensure equilibration at 300 K. Finally a 70-ps dynamics run was carried out for analysis. In the dynamics calculations, the equations of motion were solved by using the Verlet algorithm with a time step of 2 fs. The nonbonded pair list was updated every step up to a distance of 10 Å and every 10 steps for distances between 10 and 20 Å. The cutoff distance for calculation of nonbonded interactions was 20 Å. During the simulation, the temperature of the system was kept close to 300 K by coupling to a heat bath with a relaxation time of 0.1 ps (18).

RESULTS AND DISCUSSION

A very important feature that emerges from our simulation is the role played by channel waters in structure and function of gramicidinlike channels. Earlier simulations have come to similar conclusions. We find an important feature that seems to be largely characteristic of the channel itself. That is the orientation of the carbonyl and N—H dipoles and the amide plane configurations. Fig. 1 *a* shows the standard Koeppe-Kimura starting configuration in which all the carbonyl groups, and the amide planes constituting the peptide bonds, are almost exactly parallel to the long axis of the channel. In Fig. 1 *b*, which is the structure obtained by steepest descent energy minimization, it can be seen that there is a general movement of the carbonyl oxygens towards the center of the channel. Fig. 1, *c* and *d*, display the mean structures obtained from 70-ps dynamics simulations with and without the channel waters, respectively. Comparing Fig. 1, *b–d*, reveals that whereas the carbonyls move noticeably closer to the center of the channel in the dynamics averaged structure as compared to the energy minimized structure, water in the channel influences the carbonyl orientations only marginally. Only the carbonyls 14–15 and 8–9 show counter deviations between simulations with and without channel waters. Because so much of the inward motion is backbone flexing, rigid channel models would seem to be somewhat limited in their ability to describe the solvation and translocation process. The electrostatic consequence of the carbonyls pointing towards the center also helps to explain the channel's preference for cations over anions (19); there is also a high entrance barrier for anions that has been shown to be a consequence of solvation properties at the channel mouth (20).

The orientation of the N—Hs relative to the channel axis is also of considerable importance because compari-

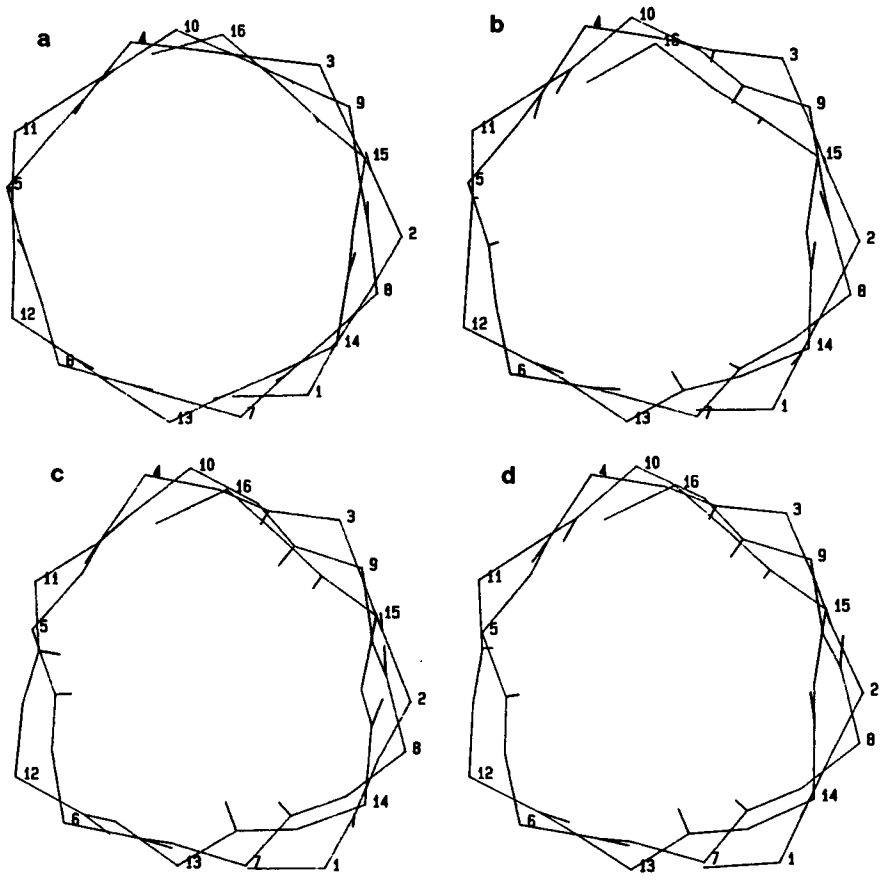

FIGURE 1. Channel backbone as seen from an end view. In addition to the backbone, the carbonyl groups are included in this representation. The numbers signify the alpha-carbons. (*a*) The starting Koeppe-Kimura regular helix with the carbonyl bonds pointing directly parallel to the channel axis. (View deviates slightly from directly down the channel axis so that the C—Os are visible.) (*b*) Structure resulting from energy minimizing the structure in *a*. (*c*) Average structure from a molecular dynamics simulation at 300° K with no waters in the channel. (*d*) is the average structure from a molecular dynamics simulation with waters in the channel and a cap of waters on each end, as described in the text.

son can be made between theoretical simulations and NMR data (21). To a fair approximation, the N—H and C—O in each amide plane are antiparallel to each other, and will hence form approximately the same angle with the long axis of the channel. In our simulations, the average orientations of the C—Os are only a few degrees different from being antiparallel to the N—Hs in the same amide plane. Also, just as the C—Os point in to the channel lumen, the N—Hs will point out from the channel lumen. The mean angle between each N—H and the long axis of the channel from the molecular dynamics simulations is shown in Fig. 2. It is seen that there is a clear alternation between the N—H angles, and with a couple of exceptions they divide roughly into two populations. One population deviates from the *z*-axis by 12–18°, and the other by 29–33°. The NMR data show two prominent peaks, one centered at 17° and the other at 40°, according to the calibration in reference 21. This is in qualitative agreement with our computed angles. An alternating pattern, as seen in Fig. 2, is also supported by recent data on NMR of individually labeled N—Hs (Cross, T. A., personal communication). It is conceivable that the computed values were smaller due to the restraints used in the simulation, which could have systematically biased the results towards the Koeppe-Kimura configuration. To test this possibility, a second set of simulations were carried out using the mean configuration, rather than the Koeppe-Kimura configuration, as the reference state. Fig. 2 *b* shows the resulting N—H orientations in comparison to the first run. They are seen to be in very close agreement. Therefore, we conclude that the final structure obtained by dynamics is not very sensitive to the precise reference structure chosen for the soft restraints. We have not carried out a simulation with the Venkatachalam-Urry structure (14) as the reference state, but the results of Fig. 2 *b* suggest that such a simulation is unlikely to make much difference in the structure obtained by dynamics.

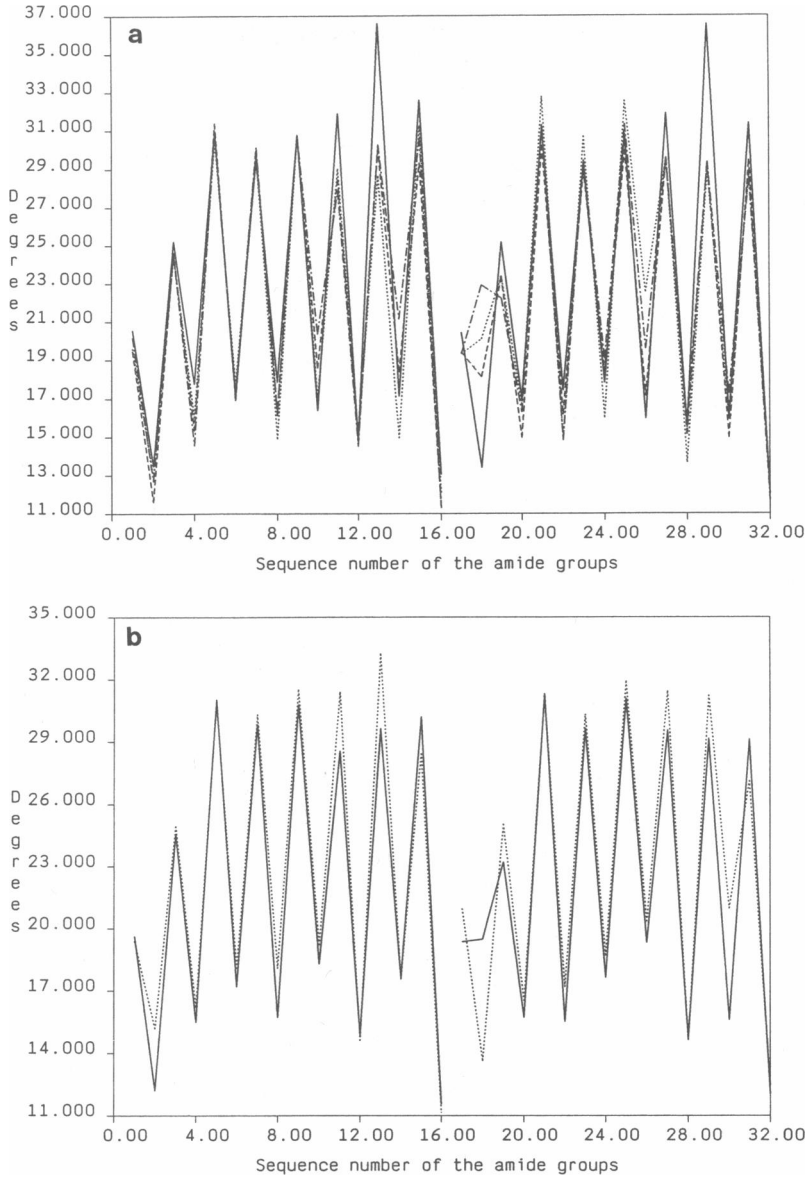

FIGURE 2. Mean angles between the N—H bonds and the long axis of the channel during molecular dynamics simulations. The N—H bonds are numbered 1–16 for each monomer, beginning at the center of the channel (valine) and going to the mouth of the channel (ethanolamine). (*a*) Solid line signifies the simulation with no waters in the channel; dotted line, the first 24 ps of our water-containing simulation before the change in water conformation (described in text); alternate dot-dash, the period from 24–34 ps while the transition was taking place; dashed line, the final period from 34–70 ps. (*b*) Solid line signifies the overall time-averaged configuration for the 70-ps run with waters in the channel and the nonelastic restraints referenced to the Koeppe-Kimura coordinates. Dashed line signifies a subsequent 35-ps run with waters in the channel and restraints referenced to the mean configuration of the previous 70-ps run.

We now consider the structure of the waters in the channel. Fig. 3 shows the time course of position along the channel axis of the oxygens of the eleven water molecules that occupy the channel during the 70-ps simulation. Eight of these, which are $\leq$ 13 Å from the center of the channel during the entire simulation, can be considered as the channel waters; the other three waters spend part of the simulation time in the channel. The figures clearly demonstrate the high degree of correlation amongst the channel waters, which makes it appropriate to consider the entire chain of waters as a single entity moving in unison. The number of conserved channel waters and the highly correlated motion are in agreement with the previous simulation results of Mackay et al. (7, 12).

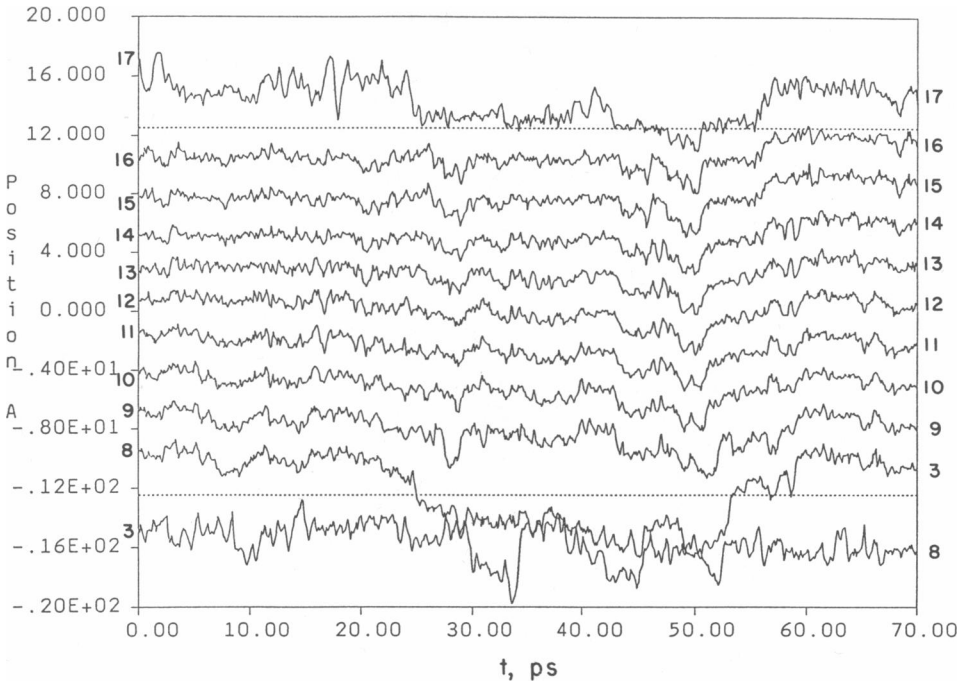

FIGURE 3. Time course of position along the channel axis of the 11 waters that are in the channel during some portion of the run. The origin is at the center of the channel and the channel mouth is judged to be 13 Å from the channel center. There are eight waters that remain in the channel during the entire simulation (9–16), and three others that spend part of the simulation in the channel (3, 8, and 17).

Another feature of the Mackay et al. results was the finding that the projections on the channel axis of the dipole moments of the channel waters had a strong tendency to point in the same direction. Our simulations show that while this oriented state is one of the low-energy states accessible to the system, there are one or more other states that are also seen. Fig. 4 *a* shows the relative projections along the channel axis of the eight waters (9–16) that are always in the channel and two other waters that spend some time in the channel. The dotted lines represent a situation where the water dipoles are precisely aligned with the channel axis. It is seen that at the beginning of the run (after equilibration) waters 8–11 have a dipole orientation in the "up" direction, whereas 13–16 have their dipole orientations in the "down" direction. Water 12 is in an intermediate or bridging dipole orientation. The nature of the "bridging" is shown in Fig. 4 *b*, which is a "snapshot" of the water configuration at 1 ps into the 70-ps dynamics run. Fig. 4 *c* shows a transition in the water structure beginning at ~31 ps into the run and complete at ~33 ps into the run. After that transition, the water has adopted the structure seen by Mackay et al. in that all the water dipoles point in the same direction along the channel axis, and remain so during the duration of the run.

The two patterns of water dipole orientation may reasonably be called different states of the system, and they are characterized by somewhat different energies. Fig. 5 *a* shows the total potential energy of the system as a function of time. Because of the noise, it is difficult to discern the energy levels of the two states and the crossing of the energy barrier between them. The noise level can be reduced by doing energy minimizations on the various conformations that are generated in time (22, 23). The results of doing energy minimizations every picosecond on the conformations that are generated in the dynamics run are given in Fig. 5 *b*. It is seen that the energy levels of the two states of water conformation and the barrier between them are made more clearly visible. The Mackay et al. conformation with all the water dipole projections along the channel axis aligned in the same direction has a higher potential energy than the earlier conformation. However we have no way to judge from these results as to which conformation has the higher free energy.

Because our molecular dynamics simulations and those of Mackay et al. are by necessity in the picosecond regime (tens of picoseconds), it is not clear as to what extent the different water conformations seen in the two simulations are caused by the differences in the models (force fields) or to what extent we happen to have sampled different regions in the total multidimensional space of possible water conformations.

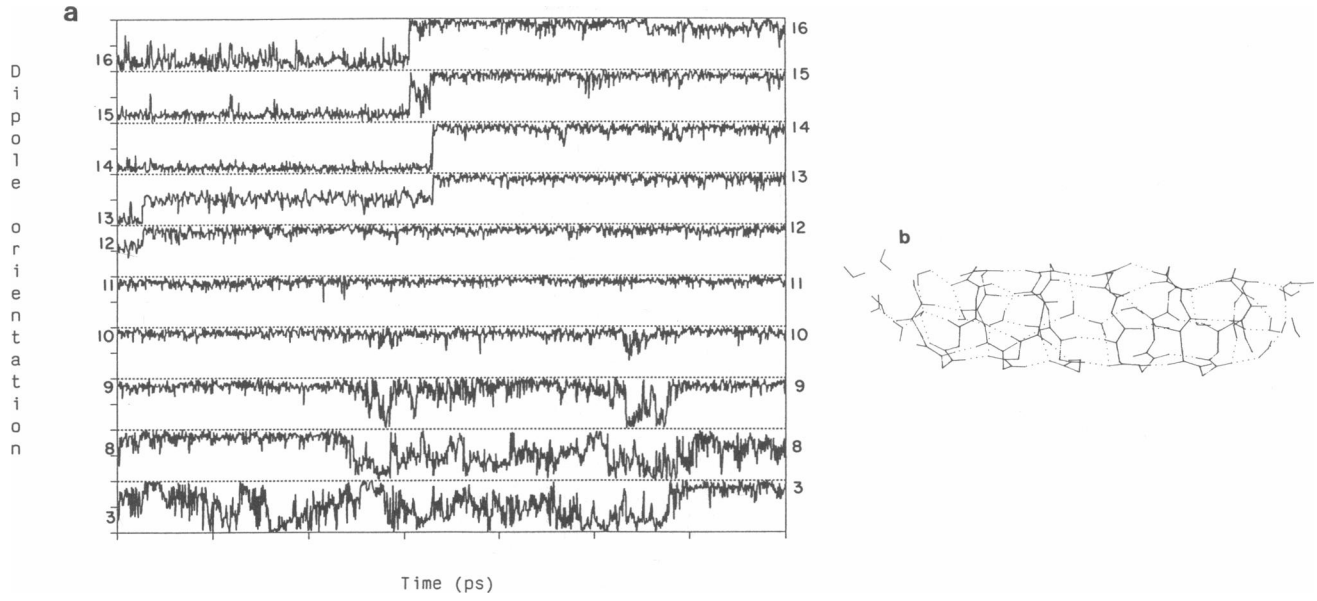

FIGURE 4. Orientation of water molecules in the channel. From top to bottom, the waters are numbers 3, and 8–16. (*a*) Normalized projection of the dipole moments along the long axis of the channel of the eight waters that are in the channel for the duration of the run, plus two waters that spend some time in the channel. For each water, the projection may vary from +1 to −1, corresponding to perfect alignment one way or the other, and represented by the dotted lines. Note the transition between 31 and 34 ps in the pattern of water dipole orientation, from a situation in which waters in each half of the channel have their dipoles oriented in opposite directions, to a subsequent pattern in which all waters are pointed in the same direction (except for a brief flipping at one end of the channel between 54 and 58 ps). (*b*) The nature of the conformation in the first part of the run, including backbone, water molecules, and hydrogen bonds. This picture is the instantaneous conformation 4 ps into the run.

Both states and the transition configuration between them are characterized by numerous water–water and water–backbone hydrogen bonds. Typically, most but not all of the waters are hydrogen bonded to each other. In addition, practically all of the waters form at least one hydrogen bond with the backbone and some form two, usually between a water hydrogen and a carbonyl oxygen. It is not possible to make any simple distinction between the states by simply counting hydrogen bonds, either in absolute terms or in the distribution between water–water

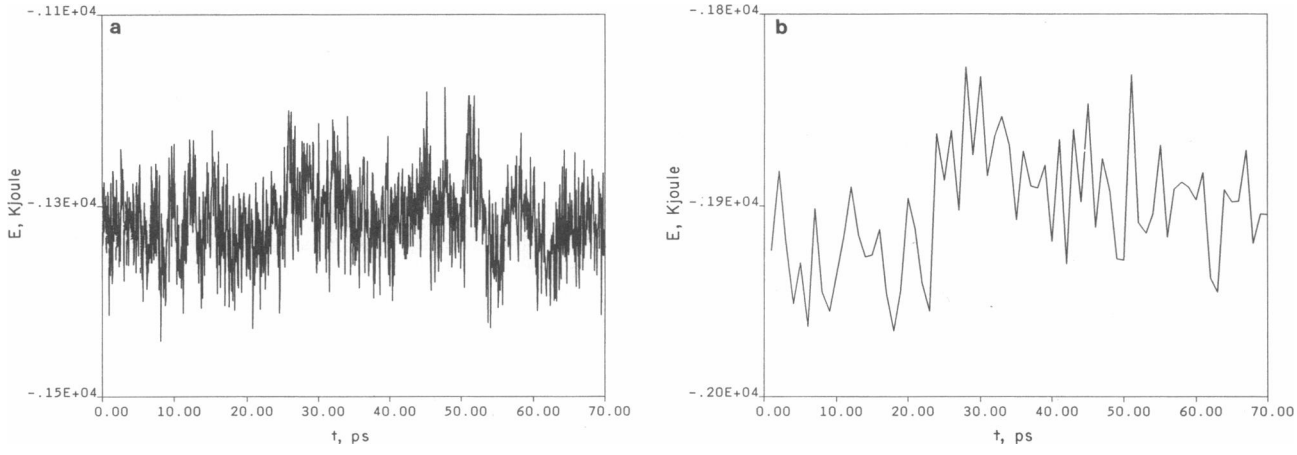

FIGURE 5. Energetics of the transition in the water pattern. (*a*) Total potential energy of the system. Although there is a lot of thermal noise, it is possible to discern the rough energy levels of the two "states" (water orientations) and the crossing of the energy barrier between them. (*b*) Quenched potential energy of the system, obtained by energy minimizing the instantaneous configurations at 2-ps intervals. Because this procedure eliminates much of the thermal noise, it is possible to see the energy levels of the two states and the energy barrier between them more clearly.

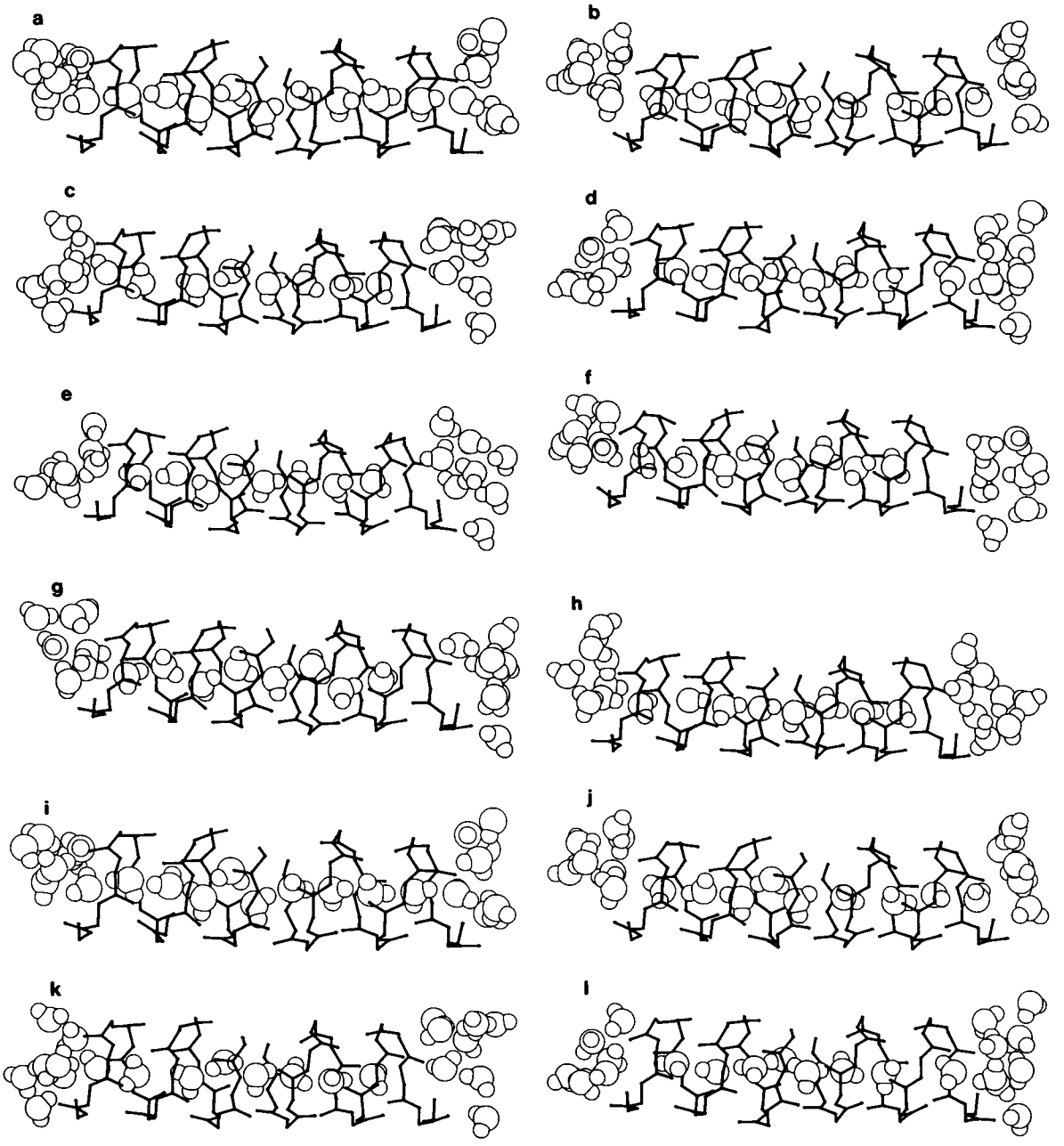

FIGURE 6. Backbone and water conformations in the two observed states and during the transition between them. (*a*) Instantaneous conformation at 20 ps (*b–g*) Conformations at 2-ps intervals from 24–34 ps. (*h*) Conformation at 40 ps. (*i–p*) Shows corresponding "quenched" (energy minimized) conformations. (Note that to the eye, the quenched conformations are not much different from the instantaneous conformations.) It appears that the beginning of the transition is marked by a water molecule leaving the left end of the channel, and that the transition itself is marked by unusually large motion as of the channel near its center. In fact one of the hydrogen bonds holding the two monomers together is broken at 28 ps: the only time that was seen during the entire run. The transition culminates in the "flipping" of the channel water dipole moments to a conformation in which they all point the same way.

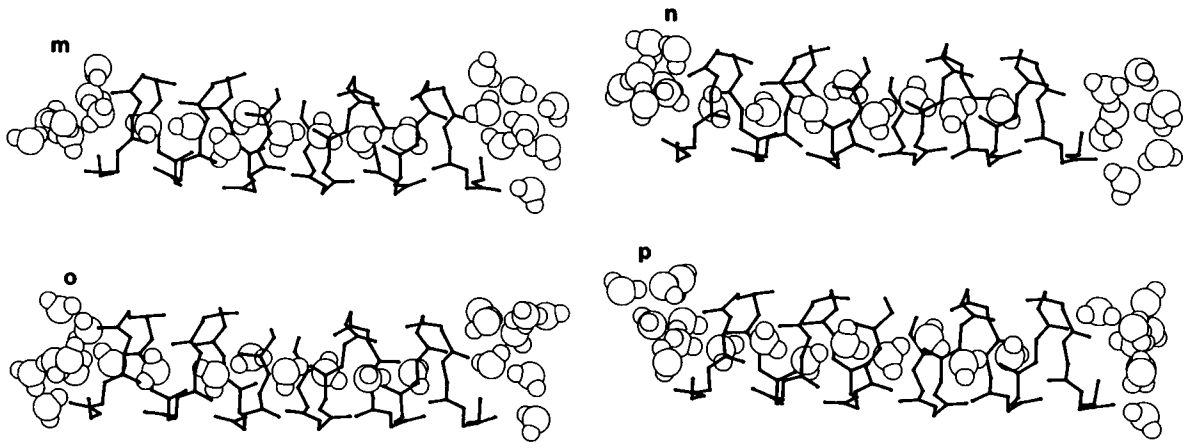

FIGURE 6. (*Continued*)

and water–backbone bonds. The energetic differences between the states seem to be more subtle than that. Fig. 6 shows protein and water conformations in the two states during the transition, both instantaneously from molecular dynamics and also after energy minimization at various time steps. The hydrogen bonding is not explicitly shown in these figures, but can easily be discerned. The sequence of events comprising the transition is notable. It appears from the "snapshot" in Fig. 6 that beginning at ~24 ps there is a momentary distortion in the structure of the channel near the junction between the monomers culminating in an actual breaking of one of the hydrogen bonds holding the dimer together (see picture at 28 ps). This distortion occurs simultaneously with a rise in the total potential energy of the structure (see Fig. 5). A third event occurs at about this time, namely an exchange of waters with the bath at the left-hand mouth of the channel. This begins at ~25 ps and is actually not complete, with the second water fully in the channel, until ~54 ps into the run (see Fig. 3). And finally, a fourth event that is involved in the transition is the "flipping" of several of the water dipole moment projections along the channel axis (see Fig. 4). The flipping begins at ~30 ps with the almost simultaneous flipping of the two waters at the right-hand channel mouth, followed at ~33 ps by the flipping of the next two waters towards the center of the channel. After that, all the water dipoles are pointed in the same direction along the channel axis for the duration of the run. The picture that naturally emerges is that the transition (between one water dipole conformation and the other) involves a coordinated motion of several parts of the channel-water system, including in this instance a distortion of the channel near the junction between the monomers and an exchange of waters between the bath and the channel at the opposite end of the channel from the end at which the water dipoles reverse the direction of their projection along the channel axis. It is likely that the reaction coordinate for ion transport is likewise a collective coordinate involving all waters and further investigation of this is in progress.

From an examination of the hydrogen bonding patterns, we find that it is very common for there to be hydrogen bonding between the water hydrogens and the carbonyl oxygens in the backbone. The orientation of the waters with the dipole moments directed mainly along the channel axis is obviously a favorable orientation for this kind of binding. This type of binding would also be enhanced by bending of the carbonyls in toward the lumen of the channel, as we observe.

CONCLUSIONS

This paper has explored the use of molecular dynamics to study the conformations of the gramicidin channel and water contained therein. We find that the channel helix has an inherent tendency to flex in such a way as to move carbonyl oxygens in towards the lumen of the channel, a tendency which is slightly enhanced by the presence of waters in the channel. The angles seen in the simulations between the backbone N—Hs and the long axis of the channel are in reasonably good agreement with NMR data. Other features emergent from the simulations include the existence of different conformational substates for the channel waters and transitions between them. The simulations also reinforce the earlier notions on the collective behavior of channel waters and point to the need for reaction coordinates involving all the waters and their principal hydrogen bonding protein partners. In future work, we will extend the simulation and analysis to the situation in which the channel contains ions and will apply time-correlation analysis to the fluctuations to

determine mobilities and detailed mechanisms for translocation through the channel.

Drs. R. E. Koeppe and D. Urry graciously provided us with details of their proposed gramicidin channel structures. Dr. T. A. Cross led us to published NMR data and shared with us unpublished NMR data on gramicidin structure.

Support for this work was received from the National Institutes of Health (grant to Dr. Jakobsson), the National Science Foundation, Robert A. Welch Foundation, Texas Advanced Research Program, (grants to Dr. McCammon), and via a grant of computer time from the National Center for Supercomputing Applications at Champaign, IL. Dr. McCammon is the recipient of the George H. Hitchings Award from the Burroughs Wellcome Fund.

Received for publication 1 December 1988 and in final form 21 April 1989.

REFERENCES

1. Jordan, P. C. 1987. Microscopic approaches to ion transport through transmembrane channels. The model system gramicidin. *J. Phys. Chem.* 91:6582–6591.
2. Hladky, S. B., and D. A. Haydon. 1984. Ion movements in gramicidin channels. Ion Channels: molecular and physiological aspects. *Curr. Top. Membr. Transp.* 21:327–363.
3. Andersen, O. S. 1984. Gramicidin channels. *Annu. Rev. Physiol.* 46:531–548.
4. Wallace, B. A. 1986. Structure of gramicidin A. *Biophys. J.* 49:295–306.
5. McCammon, J. A., and S. C. Harvey. 1987. Dynamics of Proteins and Nucleic Acids. Cambridge University Press, Cambridge, UK. 234 pp.
6. Lee, W. K., and P. C. Jordan. 1984. Molecular dynamics simulations of cation motion in water-filled gramicidin like pores. *Biophys. J.* 46:805–819.
7. Mackay, D. H. J., P. H. Berens, K. R. Wilson, and A. T. Hagler. 1984. Structure and dynamics of ion transport through gramicidin-A. *Biophys. J.* 46:229–248.
8. Kim, K. S., D. P. Vercauteren, M. Welti, S. Chin, and E. Clementi. 1985. Interaction of K^+ ion with the solvated gramicidin A transmembrane channel. *Biophys. J.* 47:327–335.
9. Roux, B., and M. Karplus. 1988. The normal modes of the gramicidin A dimer channel. *Biophys. J.* 53:297–309.
10. Skerra, A., and J. Brickman. 1987. Structure and dynamics of one-dimensional ionic solutions in biological transmembrane channels. *Biophys. J.* 51:969–975.
11. Skerra, A., and J. Brickman. 1987. Simulation of voltage-driven hydrated cation transport through narrow transmembrane channels. *Biophys. J.* 47:977–983.
12. Mackay, D. H. J., and K. R. Wilson. 1986. Possible allosteric significance of water structures in proteins. *J. Biomol. Struct. & Dyn.*, 4:491–500.
13. Koeppe, R. E., and M. Kimura. 1984. Computer building of β-helical polypeptide models. *Biopolymers.* 23:23–38.
14. Venkatachalam, C. M., and D. W. Urry. 1983. Theoretical conformational analysis of the gramicidin A transmembrane channel. I. Helix sense and energetics of head-to-head dimerization. *J. Comput. Chem.* 4:461–469.
15. Hermans, J., H. J. C. Berendsen, W. F. van Gunsteren, and J. P. M. Postma. 1984. A consistent empirical potential for water-protein interactions. *Biopolymers.* 23:1513–1518.
16. Ryckaert, J. P., G. Ciccotti, and H. J. C. Berendsen. 1977. Numerical integration of the Cartesian equations of motion of a system with constraints: molecular dynamics of *n*-alkanes. *J. Comput. Phys.* 23:327–341.
17. Hermans, J., and S. Shankar. 1986. The free energy of Xe binding to myoglobin from molecular dynamics simulation. *Isr. J. Chem.* 27:225–227.
18. van Gunsteren, W. F., and H. J. C. Berendsen. 1985. Molecular dynamics simulations: techniques and applications to proteins. *In* Molecular Dynamics and Protein Structure. J. Hermans, editor. University of North Carolina Press, Chapel Hill, NC. 5–14.
19. Myers, V. B. and D. A. Haydon. 1972. Ion transfer across lipid membranes in the presence of gramicidin A. II. The ion selectivity. *Biochim. Biophys. Acta.* 274:313–322.
20. Sung, S.-S., and P. C. Jordan. 1987. Why is gramicidin valence selective? A theoretical study. *Biophys. J.* 51:661–672.
21. Fields, G. B., C. G. Fields, J. Petefish, H. E. van Wart, and T. A. Cross. 1988. Solid phase peptide synthesis and solid-state NMR spectroscopy of [A1a3-15N][Val1] gramicidin A. *Proc. Natl. Acad. Sci. USA.* 85:1384–1388.
22. Stillinger, F. H., and T. A. Weber. 1984. Packing structures and transitions in liquids and solids. *Science (Wash. DC).* 225:983–989.
23. Elber, R., and M. Karplus. 1987. Multiple conformational states of proteins: a molecular dynamics analysis of myoglobin. *Science (Wash. DC).* 235:318–321.